ACS MATERIALS LETTERS

www.acsmaterialsletters.org

Insights of the Proton Transport Efficiency of a Membrane Electrode Assembly by Operando Monitoring of the Local Proton Concentration during Water Oxidation

Published as part of ACS Materials Letters special issue "Materials for Water Splitting".

Rajini P. Antony,[§] Lejing Li,[§] Carla Santana Santos, Ndrina Limani, Stefan Dieckhöfer, Thomas Quast, Jonas Weidner, and Wolfgang Schuhmann*

Cite This: *ACS Materials Lett.* 2024, 6, 5333−5339

ABSTRACT: **Direct estimation of the reaction environment, e.g., local pH at the anode side of a membrane electrode assembly (MEA) of zero gap electrolyzer, is essential to understand possible key factors, which are influencing the sustainable operation of industrial electrolyzers. Herein, we demonstrate a scanning electrochemical microscopy-based strategy to measure the local pH in the close vicinity of an operating MEA. Local proton concentration changes during the oxygen evolution reaction were monitored in the nonzero gap electrolyzer and MEA systems. The measurements constitute a methodology to evaluate the ion transport efficiency of the MEA. The strategy was extended to investigate the effect of an activation process, buffering of the electrolyte, and poisoning effect on the change in proton transport efficiency. This novel strategy enables the estimation of the actual pH of the MEA system during operation and is of great relevance in understanding the process conditions during sustainable fuel production.**

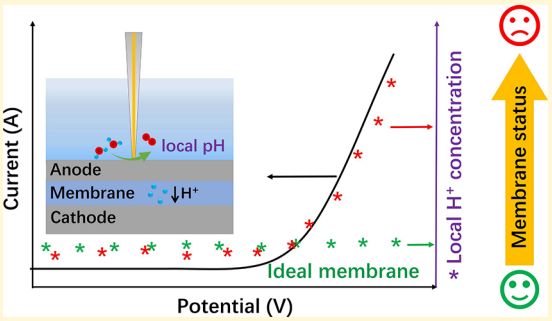

Sustainable production of fuels through renewable resources is a long-term requirement and must be operated on a large scale throughout the world to satisfy future energy demands and combat global warming. Water electrolysis is a key technology that is already available on the market. However, further scale-up is needed to address existing challenges. The stability of the employed catalysts and the improvement of energy efficiencies are the major hurdles that need to be overcome for sustainable long-term operation. The change in the local pH value at the electrode−electrolyte interface during operation, although important, is hardly discussed, and in situ measurements are challenging, especially at high current densities. Both the hydrogen evolution reaction (HER) and the oxygen evolution reaction (OER) are proton-coupled electron transfer reactions that are dependent on changes in the local pH value, e.g., by modulating the reaction kinetics.[1] In the case of proton-conducting membranes in acidic water splitting, nonzero gap electrolyzer[2] configurations and membrane electrode assembly (MEA)-based zero-gap configurations are distinguished. In the case of nonzero gap electrolyzers, at the anode side, substantial acidification is expected due to the proton liberation during the OER, and the local concentration of protons can be orders of magnitude higher during operation. A low pH value at the catalyst can influence its stability and hence affect the cell voltage and the overall performance of the electrolyzer. Moreover, the nonzero gap configuration has an efficiency loss due to electrolyte resistance due to defined spacing between the electrodes, which is minimized in the zero-gap/MEA configuration. In the MEA configuration, an optimal and efficiently working membrane would transport the protons fast enough toward the cathode side and away from the anode−electrolyte interface, which would prevent the dissolution of the employed OER catalyst and most likely mitigate local acidification.

Received: August 14, 2024
Revised: October 12, 2024
Accepted: October 14, 2024
Published: November 5, 2024

https://doi.org/10.1021/acsmaterialslett.4c01655
ACS Materials Lett. 2024, 6, 5333−5339

Therefore, knowing the local pH value at high current densities is of high importance, since it may substantially deviate in typical catalyst evaluation experiments such as, e.g., rotating-disk electrode measurements (RRDE). Any kind of catalyst and/or membrane degradation is expected to have a detrimental effect on the overall cell performance, leading to an increased cell voltage during long-term operation.[3]

The OER at the anode during water electrolysis is the rate-limiting reaction due to its sluggish kinetics. Moreover, the locally generated protons during O_2 evolution provoke local acidification, which directly influence the stability of the OER catalysts.[4,5] Geiger and co-workers introduced a metric called stability number to assess the dissolution of the Ir-based catalyst.[4] Later, Knöppel et al. studied the correlation of stability of the OER catalysts with the real pH condition of the operating MEA and emphasized the requirement of tuning and testing the catalysts in MEA configuration.[3] Thus, local acidification may hamper the long-term operation of the electrolyzer.

For this reason, the balance between the proton production during the OER and the proton transport through the membrane from the vicinity of the catalysts toward the cathode side of the MEA needs to be verified in both nonzero gap electrolyzer and MEA systems. This is essential to develop an improved understanding of the local acidification effect, as well as potential catalyst and membrane permeability degradation. Membrane degradation may be caused by mechanical, thermal, or chemical means, which will result in membrane thinning, pinhole formation, and a decrease in proton conductivity.[6−8] Probing the proton concentration at the anode-electrolyte interface can hence provide vital information about the integrity of the membrane and catalysts.

Substantial efforts have been made in probing the interfacial pH which includes techniques such as RRDE,[9,10] fluorescence spectroscopy,[11,12] micro-Raman spectroscopy,[13,14] and scanning electrochemical microscopy (SECM).[15−17] However, fluorescence spectroscopy and micro-Raman spectroscopy face limitations, such as the requirement of pH-sensitive fluorophores, which are stable in the electrolyte as well as a response in the pH range of interest. SECM has been explored to measure the local pH changes in the proximity of operating electrode surfaces during HER,[10] OER,[17] and the CO_2 reduction reaction.[18] We recently demonstrated the use of Au nano- and microelectrodes combined with shear-force mode SECM positioning to determine the local pH during the OER, which provides the advantage of sensing the pH in a broad range even at high acidic conditions and simultaneously avoiding interference from the oxygen reduction reaction (ORR) at the gold microelectrode.[17] These measurements were performed with electrodes immersed in the electrolyte solution in front of the catalyst-modified surface and hence monitoring changes in interfacial properties, e.g., the pH value. In the case of a MEA system, where the produced protons are expected to be transported through the cation-conducting membrane to the cathode side of the MEA, the level of local acidification was unknown.

We evaluated the local proton concentration in the vicinity of the IrO_2 side of a MEA in two different cell configurations, separately, i.e., the placement of the counter electrode is different for the two cell configurations. Specifically, Scheme 1a shows the configuration in which the Pt cathode side of the MEA itself is connected as counter electrode in a 3-electrode setup including a reference electrode. This setup resembles a zero-gap electrolyzer. In this case, we would expect that most of the protons liberated during the OER are transported through the Nafion membrane to be reduced at the Pt side of the MEA. In contrast, Scheme 1b resembles an IrO_2 side of a MEA immersed in an electrolyte in a nonzero-gap situation with an external counter electrode located in the same electrolyte compartment. In this case, no proton gradient through the underlying cation-exchange Nafion membrane is established during the OER, and it is hence anticipated that the liberated protons are diffusing from the IrO_2 catalyst interface into the electrolyte solution and toward the external counter electrode. Therefore, a distinct difference in the local acidification at the anode-electrolyte interface is expected for the two different configurations shown in Scheme 1. The quantification of the proton concentration was performed by positioning a Au microelectrode in the immediate vicinity of the anode while applying potentials sufficiently high for the OER. By investigating the proton concentration in the vicinity of the IrO_2 side using the same MEA but differently connected counter electrodes, we can evaluate the proton transport efficiency through the membrane.

Scheme 1. Schematic of the Two Configurations Explored in the Study[a]

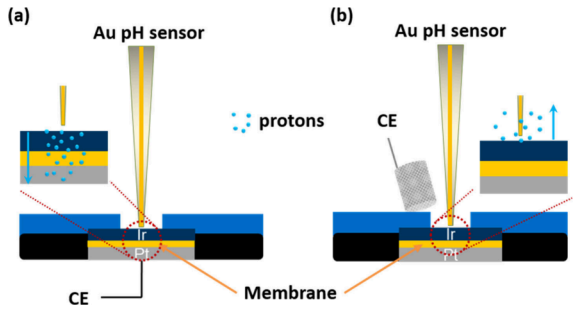

[a](a) Zero gap electrolyzer (MEA) where the counter electrode is the cathode of the MEA and (b) nonzero gap electrolyzer, where the counter electrode is an external Pt mesh positioned in the electrolyte. Note the Au pH sensor is positioned in very close proximity of the anode surface using SECM positioning. The blue arrow in the zoom-in figure represents the movement direction of protons.

We further explored these two configurations to investigate the effects of membrane activation by hydrating as well the influence of a buffer electrolyte to prevent large local pH changes during operation. To the best of our knowledge, no attempts have been disclosed reporting changes in the local pH in the proximity of the anode/electrolyte interface in an operating MEA system in pure water. Finally, by actively inducing chemical membrane degradation, we emphasized studying how membrane degradation impacts cell performance. The effect of chemical degradation on the proton conductivity of MEA was evaluated indirectly by probing the change in the local proton concentration using the proposed local pH determination methodology by comparing activated and poisoned MEA systems.

Similar to the approach proposed in our previous report,[17] in this work we used a microelectrode with a gold disc to record voltammograms to provoke the oxidation of Au followed by the Au−O_x reduction. The changes in local acidification of the electrolyte were calculated by monitoring the shift of the Au−O_x reduction peak potential in the Au ultramicroelectrode (UME) cyclic voltammograms, with the Au UME being positioned in close proximity to the anode side of the MEA.

https://doi.org/10.1021/acsmaterialslett.4c01655
ACS Materials Lett. 2024, 6, 5333−5339

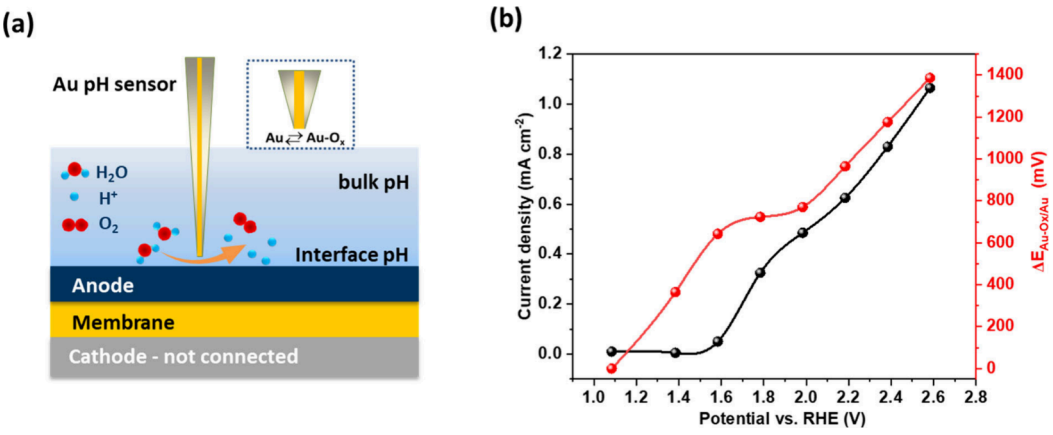

Figure 1. (a) Schematic of probing the proton concentration in a nonzero gap electrolyzer system by means of a Au microelectrode and (b) changes in current density and proton concentration measured in terms of $\Delta E_{\text{Au-Ox/Au}}$ as a function of the applied potential on the anode side using the nonzero gap electrolyzer system.

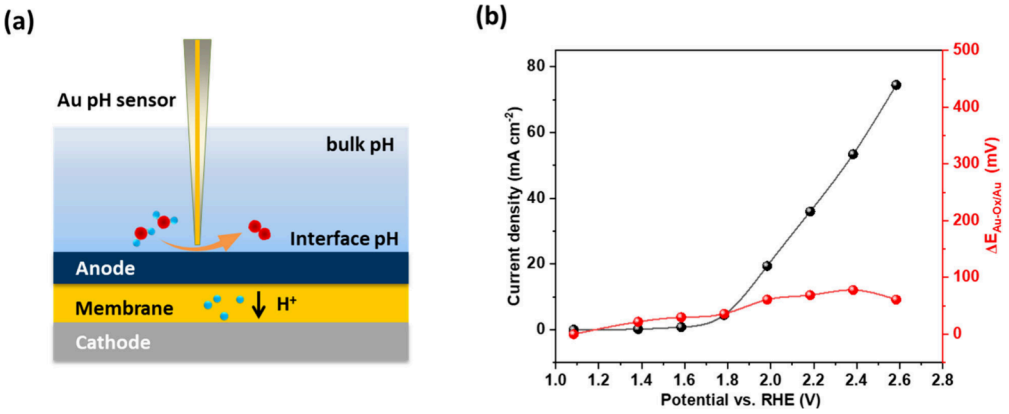

Figure 2. (a) Schematic of probing the local proton concentration in MEA configuration by using an Au microelectrode; and (b) recorded current density and corresponding change in the local proton concentration displayed in terms of $\Delta E_{\text{Au-Ox/Au}}$ as a function of the applied potential on the anode side of the MEA. The counter electrode is the MEA cathode (Pt) separated by the membrane from the polarized anode.

The morphologies of the anode and cathode side of the commercial MEA are shown in Figure S1. The SECM-based setup for local pH studies at an operating MEA is shown in Figure S2.

Before the local pH measurement, a calibration curve was made by registering voltammograms using Au UME in electrolytes with a known proton concentration (Figure S3). More details on the calibration procedures and Au probe dimensions (Figure S4) are provided in the SI (experimental section). In the nonzero gap system, the local proton concentrations in dependence on the applied potentials at the MEA anode were measured by positioning the Au UME close to the anode (Figure 1a). With increasing current density at higher applied potentials due to the increasing OER, the Au−O_x/Au reduction peak potential positions shifted in correspondence with the local proton concentration. Note: The data are representing a relative shift in the Au−O_x/Au reduction peak potential, starting from the peak potential observed during polarization of the sample at a resting potential at which no OER occurs (V_{rest} = 1.19 V vs RHE). Changes of the peak potential ($\Delta E_{\text{Au-Ox/Au}}$) were used due to exceeding the pH scale, which requires consideration of water and proton activities (see also SI for more information). Therefore, we show the data in Figure 1b as the relative shift of the Au−O_x/Au reduction peak potential since the water activity decreases due to undercoordination at extremely high proton concentrations, which must be considered in the corresponding Nernst equation. The results in Figure 1b indicate that, at high anodic potential (>2.0 V vs RHE), the OER imposed a modulation of the local proton concentration even exceeding 9.7 M, which is beyond the calibration regime. The results are demonstrating the presumed high local acidification at the catalyst−electrolyte interface in dependence of the OER,[3] which might be responsible for the dissolution of the Ir-based catalyst[3] in nonzero gap configurations. This questions the transferability of typical catalyst characterization procedures such as rotating-disk or rotating-ring-disk voltammetry to the conditions in nonzero gap electrolyzers.

The use of a buffer in the electrolyte was reported to be effective in electrolysis processes at near-neutral pH conditions.[1,14,19] In the presence of a buffer, the local pH should remain constant at the electrode interface, increasing the performance compared to the unbuffered system. To evaluate the buffer effect in terms of stabilizing the local pH during the OER, we determined the local pH in the vicinity of an operating OER electrode in the presence of phosphate buffer solution (0.1 M, pH 7).[20] An experiment in the nonzero gap electrolyzer configuration was performed using the buffer

https://doi.org/10.1021/acsmaterialslett.4c01655
ACS Materials Lett. 2024, 6, 5333−5339

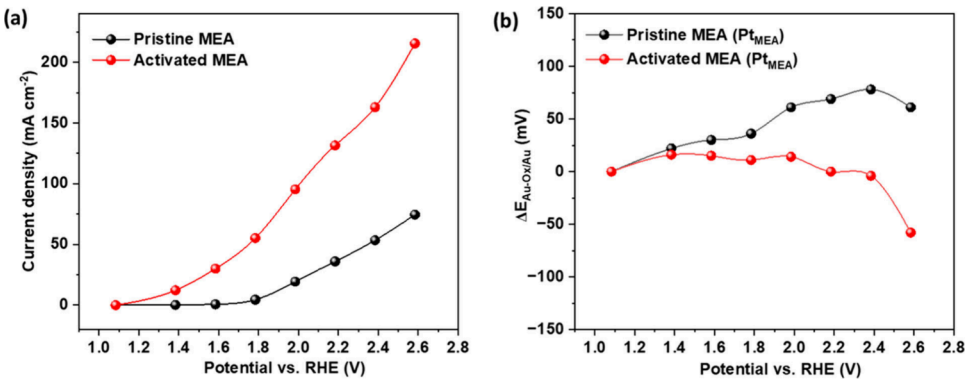

Figure 3. (a) Substrate potential dependent current densities for a pristine and an activated MEA in zero-gap electrolyzer configuration, i.e., counter electrode is the Pt cathode separated by the membrane from the polarized anode. (b) Change in the local proton concentration as a function of the applied potential in a zero-gap electrolyzer. All measurements were carried out in water.

electrolyte. As anticipated, an improvement in the catalytic current was observed (Figure S5a), demonstrating that the proton concentration gradient can be modulated, and the buffer capacity was sufficient to decrease the local pH shift when the sample was polarized in a potential window of 1.0 to 1.8 V vs RHE (Figure S5b). At potentials beyond 1.8 V, the buffer capacity of the used phosphate buffer was insufficient to maintain the local proton concentrations which decreased by about ∼40%. Evidently, the presence of a buffer cannot eliminate the shift of the local proton concentration at high current densities in the nonzero gap electrolyzer configuration.

In contrast, when the MEA Pt-cathode is connected as a counter electrode (Scheme 1a), the anode and the cathode are only separated by a proton-conducting membrane. Although many publications indicate a possible high proton concentration and its effect during electrolyzer operation, a sound investigation is necessary to ascertain the difference in the local electrolyte acidification in a nonzero gap electrolyzer and in MEA configuration. The proton transport can then take place through the proton-conducting Nafion membrane (Figure 2a), and even if polarized to high anodic potentials the detected local proton concentration does not change (Figures 2b, S6) due to high proton conducting property of the pristine Nafion membrane. Interestingly, the current density was higher using the MEA configuration than in the nonzero gap electrolyzer. We anticipate that the low conductivity of pure water was the main factor causing a lower current in the nonzero gap electrolyzer configuration.

After an induction period of hours to days performing water splitting in the MEA configuration, the activity improved and reached an optimum and stable performance. This is in accordance with previous reports, in which it is well documented that different types of conditioning protocols are necessary to improve the activity in terms of the required overpotential at a given current density.[21,22] This activation process may contribute to dissolve impurities present in the MEA, to activate catalytic sites, and to completely hydrate the MEA to facilitate the transfer of reactants. Hydration might require a few hours to days to reach equilibrium.[23]

Based on these observations, an activation protocol was established (Figure S7) for a pristine MEA, in which the MEA was subjected to a galvanostatic pulse sequence with periodic changes in the polarization to 50 mA cm^{-2} followed by a relaxation period (no polarization). After activation, the MEA was washed and transferred into the SECM cell for evaluating the OER activity, as described above. The activated MEA performance improved, as seen in the higher current density at a lower applied potential compared to the pristine MEA (Figure 3a). The observed increased current density is attributed to the formation of channels in the MEA for facilitating the mass transport of ions, gases, and liquids, the hydration of the Nafion membrane and the Nafion network in the catalyst layer, as well as the removal of contaminants.[22] A positive ΔE indicates an increase in proton concentration, and a negative ΔE corresponds to a decrease in proton concentration. For the activated MEA, the corresponding changes in the local proton concentration were indeed smaller compared with that of the pristine MEA in the E_{sub} range from 1.40 to 2.58 V vs RHE (Figure 3b). This can be attributed to an effective bubble distribution[24] and the fast mixing of the electrolyte adjacent to the electrode which reduces acidification.

These results suggest that the proposed methodology may be advantageously applied to monitor the proton transport efficiency through the ion-conducting membrane in a MEA system. We hypothesize that local pH measurements at the anode surface could be the basis to investigate the influence of possible membrane degradation onto the proton transport capability through the membrane. It is known that the proton conductivity of the membrane can decay due to degradation processes, such as exposure to high temperature or ion blocking effects.[25] This in turn leads to a deficiency of protons at the cathode and in consequence to a lower overall water electrolysis performance.[26] Moreover, simultaneous local acidification at the anode side will accelerate catalyst degradation. An initial indication is the current density where we observed a drastic increase or decrease in the current density values after activation of the membrane or subjecting the membrane to a treatment to highly active oxygen radicals generated by means of Fenton's reaction, respectively. This change in current density could be induced by changing the properties of both catalysts and membrane. Catalyst poisoning and/or a decrease in membrane proton conductivity are assumed to be the major parameters contributing to this. Hence, we used the proposed methodology to determine the local pH value to assess the proton transport ability of the MEA system, since any degradation or blocking effect in the membrane and/or catalyst layer of MEA will be reflected as a change in the local proton concentration at the anode-electrolyte interface (Figure 4a). To evaluate the

https://doi.org/10.1021/acsmaterialslett.4c01655
ACS Materials Lett. 2024, 6, 5333−5339

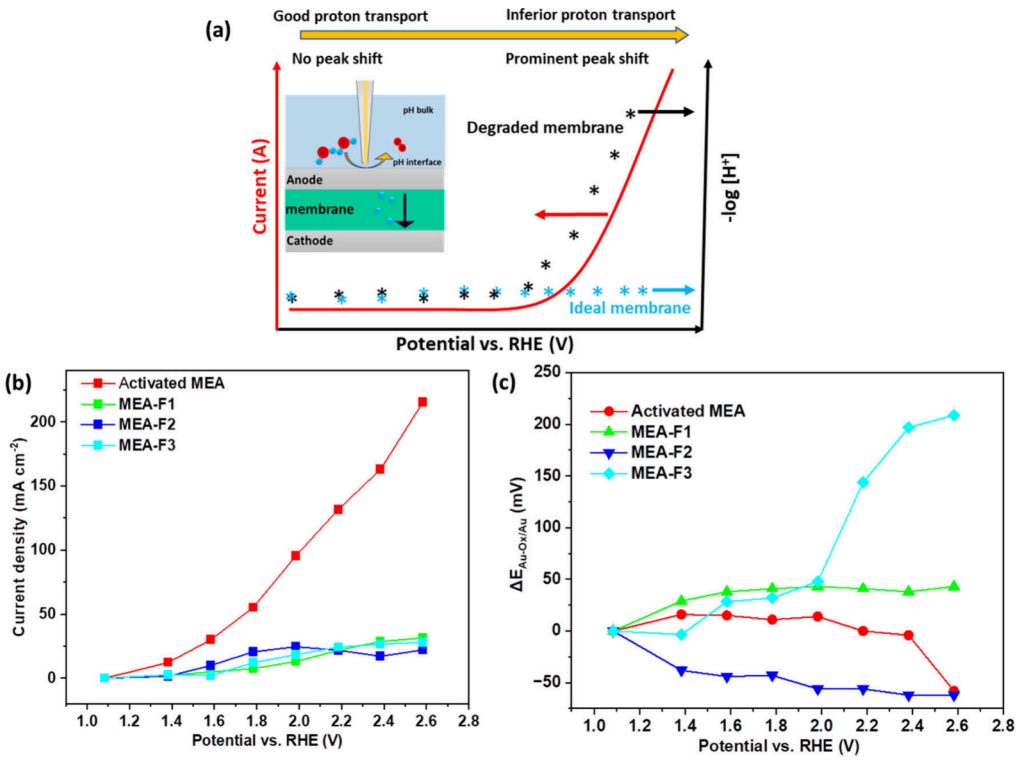

Figure 4. (a) Schematic showing the correlation of local pH changes due to membrane degradation and the resulting changes in the proton transport capabilities. The measurements were carried out in MEA configuration using the MEA cathode as counter electrode. (b) Change in OER current density as a function of substrate potential for MEAs treated for different time intervals in Fenton's solution. (c) Shift of $\Delta E_{Au\text{-}Ox/Au}$ as a function of the applied potential on the anode side.

degradation of the MEA, an active accelerated degradation was chosen based on a Fenton's process to locally create radicals which can degrade the Nafion polymer structure.[27] The Fenton's degradation process is explained in more detail in the Supporting Information (Figure S8a). The membrane degradation was monitored with individual MEAs which were subjected to different durations of exposure to the Fenton's solution for 2 h (MEA-F1), 24 h (MEA-F2), 1 week (MEA-F3), respectively. Afterward, the MEAs were washed to remove any excess of Fe ions trapped inside the membrane. Figure S8 shows the photographs of a MEA during and after the Fenton's treatment. The SECM-based local proton concentration determination was performed in the zero-gap MEA electrolyzer configuration. A significant decrease in the current density after the Fenton's process was evident for all samples irrespective of their immersion time into the Fenton's solution, as depicted in Figure 4b. This may be attributed to a poisoning effect, which can decrease the catalytic activity. In addition, the Fe^{3+} formed during Fenton's process can bind with the sulfonate groups and block the proton sites in the membrane and thus can decrease the proton conductivity. With an increase in the immersion time of the MEA in the Fenton's reagent, more catalytic sites are poisoned with Fe ions and the radicals produced during Fenton's process can damage the polymer backbone of the Nafion membrane, causing a decrease in the proton transport activity, which is reflected by the decrease in the current density during zero-gap MEA electrolyzer operation.

Interestingly, the position of the Au−O_x/Au reduction peak potential did not substantially shift for the MEA samples treated for up to 24 h (MEA-F2). However, a clear deviation of the local proton concentration was observed for MEA-F3, which was exposed to the Fenton's process for 1 week (Figure 4c) at potentials exceeding 2.0 V vs RHE. This acidification at the anode interface reveals that the protons could not efficiently be transferred from the anode to the cathode side, suggesting a degradation of the MEA membrane and impacting on the proton transport channels after the extensive Fenton's treatment. In the case of MEA-F1 and MEA-F2, the Fentons's process exhibits insignificant impact on the proton transport efficacy, and the blocked sites in the membrane by Fe^{3+} ions could be efficiently exchanged by protons at higher current densities. After 1 week of Fenton's process, the membrane damage by excess radical formation is irreversible and permeation of protons is impaired leading to a local acidification at the anode surface as detected by the positioned Au UME.

In summary, we successfully established an SECM based *operando*-electrochemical methodology to probe the actual local pH value at the anode-electrolyte interface during overall water electrolysis in a MEA configuration. Probing, for comparison, the local proton concentration at a MEA in two configurations, namely in a nonzero gap configuration with the counter electrode located in the electrolyte above the anode and a MEA configuration using the MEA cathode as counter electrode, enabled us to assess the proton transport ability through the membrane during operation. The effect of an activation process, buffering the electrolyte, and chemical degradation of the membrane onto the proton conductivity of the MEA was investigated via probing the local proton concentrations in proximity of the operating anode. By comparing activated and poisoned MEAs we could demonstrate the capability of the proposed method for characterizing water splitting in an operating MEA electrolyzer systems,

https://doi.org/10.1021/acsmaterialslett.4c01655
ACS Materials Lett. 2024, 6, 5333−5339

which is crucial for developing future proton exchange membrane-based electrolyzers.

■ ASSOCIATED CONTENT

Supporting Information

The Supporting Information is available free of charge at https://pubs.acs.org/doi/10.1021/acsmaterialslett.4c01655.

Full experimental procedures and additional figures (PDF)

■ AUTHOR INFORMATION

Corresponding Author

Wolfgang Schuhmann − *Analytical Chemistry—Center for Electrochemical Sciences (CES), Faculty of Chemistry and Biochemistry, Ruhr University Bochum, D-44780 Bochum, Germany;* orcid.org/0000-0003-2916-5223; Email: wolfgang.schuhmann@rub.de

Authors

Rajini P. Antony − *Analytical Chemistry—Center for Electrochemical Sciences (CES), Faculty of Chemistry and Biochemistry, Ruhr University Bochum, D-44780 Bochum, Germany;* Present Address: Water and Steam Chemistry Division, Bhabha Atomic Research Centre Facilities, Kalpakkam, Tamilnadu 603102, India

Lejing Li − *Analytical Chemistry—Center for Electrochemical Sciences (CES), Faculty of Chemistry and Biochemistry, Ruhr University Bochum, D-44780 Bochum, Germany*

Carla Santana Santos − *Analytical Chemistry—Center for Electrochemical Sciences (CES), Faculty of Chemistry and Biochemistry, Ruhr University Bochum, D-44780 Bochum, Germany*

Ndrina Limani − *Analytical Chemistry—Center for Electrochemical Sciences (CES), Faculty of Chemistry and Biochemistry, Ruhr University Bochum, D-44780 Bochum, Germany*

Stefan Dieckhöfer − *Analytical Chemistry—Center for Electrochemical Sciences (CES), Faculty of Chemistry and Biochemistry, Ruhr University Bochum, D-44780 Bochum, Germany*

Thomas Quast − *Analytical Chemistry—Center for Electrochemical Sciences (CES), Faculty of Chemistry and Biochemistry, Ruhr University Bochum, D-44780 Bochum, Germany*

Jonas Weidner − *Analytical Chemistry—Center for Electrochemical Sciences (CES), Faculty of Chemistry and Biochemistry, Ruhr University Bochum, D-44780 Bochum, Germany*

Complete contact information is available at: https://pubs.acs.org/10.1021/acsmaterialslett.4c01655

Author Contributions

[§]Rajini P Antony and Lejing Li contributed equally. CRediT: **Rajini P. Antony** conceptualization, data curation, formal analysis, investigation, methodology, validation, writing - original draft, writing - review & editing; **Lejing Li** conceptualization, data curation, formal analysis, investigation, methodology, writing - original draft, writing - review & editing; **Carla Santana Santos** data curation, methodology, validation, writing - original draft, writing - review & editing; **Ndrina Limani** data curation, investigation, writing - review & editing; **Stefan Dieckhöfer** investigation, methodology, validation; **Thomas Quast** investigation, methodology, validation; **Jonas Weidner** investigation, methodology; **Wolfgang Schuhmann** conceptualization, funding acquisition, project administration, resources, supervision, writing - review & editing.

Notes

The authors declare no competing financial interest.

■ ACKNOWLEDGMENTS

This work was in part financially supported by the European Research Council (ERC) under the European Union's Horizon 2020 research and innovation programme (CasCat [833408]); by the European Union's Horizon Europe research and innovation programme—European Innovation Council (EIC) under grant agreement No 101046742 (MeBattery); by the Bundesministerium für Forschung und Technology (BMBF) in the framework of the project "DERIEL" [03HY122H]; as well as the Deutsche Forschungsgemeinschaft (DFG) in the framework of the CRC247 [388390466].

■ REFERENCES

(1) Obata, K.; van de Krol, R.; Schwarze, M.; Schomäcker, R.; Abdi, F. F. In situ observation of pH change during water splitting in neutral pH conditions: impact of natural convection driven by buoyancy effects. *Energy Environ. Sci.* **2020**, *13* (12), 5104.

(2) Ehelebe, K.; Escalera-López, D.; Cherevko, S. Limitations of aqueous model systems in the stability assessment of electrocatalysts for oxygen reactions in fuel cell and electrolyzers. *Curr. Opin. Electrochem.* **2021**, *29*, 100832.

(3) Knöppel, J.; Möckl, M.; Escalera-López, D.; Stojanovski, K.; Bierling, M.; Böhm, T.; Thiele, S.; Rzepka, M.; Cherevko, S. On the limitations in assessing stability of oxygen evolution catalysts using aqueous model electrochemical cells. *Nat. Commun.* **2021**, *12* (1), 2231.

(4) Geiger, S.; Kasian, O.; Ledendecker, M.; Pizzutilo, E.; Mingers, A. M.; Fu, W. T.; Diaz-Morales, O.; Li, Z.; Oellers, T.; Fruchter, L.; Ludwig, A.; Mayrhofer, K. J. J.; Koper, M. T. M.; Cherevko, S. The stability number as a metric for electrocatalyst stability benchmarking. *Nat. Catal.* **2018**, *1* (7), 508−515.

(5) Chen, F.-Y.; Wu, Z.-Y.; Adler, Z.; Wang, H. Stability challenges of electrocatalytic oxygen evolution reaction: From mechanistic understanding to reactor design. *Joule* **2021**, *5* (7), 1704−1731.

(6) Luo, X.; Ghassemzadeh, L.; Holdcroft, S. Effect of free radical-induced degradation on water permeation through PFSA ionomer membranes. *Int. J. Hydrogen Energy* **2015**, *40* (46), 16714−16723.

(7) Hongsirikarn, K.; Mo, X.; Goodwin, J. G.; Creager, S. Effect of H_2O_2 on Nafion properties and conductivity at fuel cell conditions. *J. Power Sources* **2011**, *196* (6), 3060−3072.

(8) Chandesris, M.; Médeau, V.; Guillet, N.; Chelghoum, S.; Thoby, D.; Fouda-Onana, F. Membrane degradation in PEM water electrolyzer: Numerical modeling and experimental evidence of the influence of temperature and current density. *Int. J. Hydrogen Energy* **2015**, *40* (3), 1353−1366.

(9) Yokoyama, Y.; Miyazaki, K.; Miyahara, Y.; Fukutsuka, T.; Abe, T. In Situ Measurement of local pH at working electrodes in neutral pH Solutions by the rotating ring-disk electrode technique. *ChemElectroChem.* **2019**, *6* (18), 4750−4756.

(10) Monteiro, M. C. O.; Liu, X.; Hagedoorn, B. J. L.; Snabilié, D. D.; Koper, M. T. M. Interfacial pH measurements using a rotating ring-disc electrode with a voltammetric pH sensor. *ChemElectroChem.* **2022**, *9* (1), No. e202101223.

(11) Bowyer, W. J.; Xie, J.; Engstrom, R. C. Fluorescence imaging of the heterogeneous reduction of oxygen. *Anal. Chem.* **1996**, *68* (13), 2005−2009.

(12) Leenheer, A. J.; Atwater, H. A. Imaging water-splitting electrocatalysts with pH-sensing confocal fluorescence microscopy. *J. Electrochem. Soc.* **2012**, *159* (9), H752−H757.
(13) Lackey, H. E.; Nelson, G. L.; Lines, A. M.; Bryan, S. A. Reimagining pH measurement: Utilizing Raman spectroscopy for enhanced accuracy in phosphoric acid systems. *Anal. Chem.* **2020**, *92* (8), 5882−5889.
(14) Lu, S.; Zhang, Z.; Zhang, B.; Shi, Y. Insight into the change in local pH near the electrode surface using phosphate species as the probe. *J. Phys. Chem. Lett.* **2023**, *14* (46), 10457−10462.
(15) Monteiro, M. C. O.; Jacobse, L.; Touzalin, T.; Koper, M. T. M. Mediator-free SECM for probing the diffusion layer ph with functionalized gold ultramicroelectrodes. *Anal. Chem.* **2020**, *92* (2), 2237−2243.
(16) Monteiro, M. C. O.; Mirabal, A.; Jacobse, L.; Doblhoff-Dier, K.; Barton, S. C.; Koper, M. T. M. Time-resolved local pH measurements during CO_2 reduction using scanning electrochemical microscopy: Buffering and tip effects. *JACS Au* **2021**, *1* (11), 1915−1924.
(17) Li, L.; Limani, N.; P Antony, R.; Dieckhöfer, S.; Santana Santos, C.; Schuhmann, W. Au micro- and nanoelectrodes as local voltammetric pH sensors during oxygen evolution at electrocatalyst-modified electrodes. *Small Sci.* **2024**, *4*, 2300283.
(18) Dieckhöfer, S.; Öhl, D.; Junqueira, J. R. C.; Quast, T.; Turek, T.; Schuhmann, W. Probing the local reaction environment during high turnover carbon dioxide reduction with Ag-based gas diffusion electrodes. *Chem.—Eur. J.* **2021**, *27* (19), 5906−5912.
(19) Shinagawa, T.; Takanabe, K. Electrocatalytic hydrogen evolution under densely buffered neutral pH conditions. *J. Phys. Chem. C* **2015**, *119* (35), 20453−20458.
(20) Naito, T.; Shinagawa, T.; Nishimoto, T.; Takanabe, K. Water electrolysis in saturated phosphate buffer at neutral pH. *ChemSusChem* **2020**, *13* (22), 5921−5933.
(21) Lim, A.; Kim, H.-j.; Henkensmeier, D.; Jong Yoo, S.; Young Kim, J.; Young Lee, S.; Sung, Y.-E.; Jang, J. H.; Park, H. S. A study on electrode fabrication and operation variables affecting the performance of anion exchange membrane water electrolysis. *J. Ind. Eng. Chem.* **2019**, *76*, 410−418.
(22) Taghiabadi, M. M.; Zhiani, M.; Silva, V. Effect of MEA activation method on the long-term performance of PEM fuel cell. *Appl. Energy* **2019**, *242*, 602−611.
(23) Christmann, K.; Friedrich, K. A.; Zamel, N. Activation mechanisms in the catalyst coated membrane of PEM fuel cells. *Prog. Energy Combust. Sci.* **2021**, *85*, 100924.
(24) Wang, W.; Li, K.; Ding, L.; Yu, S.; Xie, Z.; Cullen, D. A.; Yu, H.; Bender, G.; Kang, Z.; Wrubel, J. A.; Ma, Z.; Capuano, C. B.; Keane, A.; Ayers, K.; Zhang, F.-Y. Exploring the impacts of conditioning on proton exchange membrane electrolyzers by in situ visualization and electrochemistry characterization. *ACS Appl. Mater. Interface* **2022**, *14* (7), 9002−9012.
(25) Li, N.; Araya, S. S.; Cui, X.; Kær, S. K. The effects of cationic impurities on the performance of proton exchange membrane water electrolyzer. *J. Power Sources* **2020**, *473*, 228617.
(26) Li, N.; Araya, S. S.; Kær, S. K. Long-term contamination effect of iron ions on cell performance degradation of proton exchange membrane water electrolyser. *J. Power Sources* **2019**, *434*, 226755.
(27) Kundu, S.; Simon, L. C.; Fowler, M. W. Comparison of two accelerated Nafion degradation experiments. *Polym. Degrad. Stab.* **2008**, *93* (1), 214−224.

https://doi.org/10.1021/acsmaterialslett.4c01655
ACS Materials Lett. 2024, 6, 5333−5339